VERSITA

OPTO-ELECTRONICS REVIEW **14**(4), 275–279

DOI: 10.2478/s11772-006-0036-7

Nonlinear optical properties of composites based on conductive metal-alkanoate liquid crystals

S. BUGAYCHUK*[1], G. KLIMUSHEVA[1], Y. GARBOVSKIY[1], T. MIRNAYA[2], and A. ISCHENKO[3]

[1]Institute of Physics, 46 Nauki Str., 03-028 Kiev, Ukraine
[2]Institute of General and Inorganic Chemistry, 32/34 Palladina Ave., 03-142 Kiev, Ukraine
[3]Institute of Organic Chemistry, 5 Murmanskaya Str., 02-142 Kiev, Ukraine

The dynamic holography in new composite materials based on a novel class of metal-alkanoate ionic liquid crystals (ILCs) is studied experimentally and theoretically. The composites are formed as a dielectric dye film covered by lyotropic metal-alkanoate ILC and ionic smectic glasses with doped dye molecules. The dynamic gratings are created by nanosecond pulses of double frequency Nd:YAP laser, the recording demonstrates fast erasure time of residual thermal gratings. The nonlinear optical properties are determined by the resonance nonlinearity in photosensitive centres of ILC. Note, that permanent relief gratings will be formed on a dielectric dye film only as well as in composite cells either with nematic LC or with polymers under action of pulsed laser radiation. Lyotropic ILC layer applied over the dye film provides the dynamic regime of grating recording in composite cells. We found a secondary thermal grating is much smaller, the conductive ILC matrix provides effective heat dissipation and erasure of this thermal grating. A theory of Raman-Nath self-diffraction holography on thin films followed from the wave equation and the nonlinear mechanism of absorption saturation is developed to explain experimental results.

Keywords: ionic liquid crystals, dynamic holographic recording, composites.

1. Introduction

Class of ionic liquid crystals (ILCs) based on metal alkanoates includes lyotropic and thermotropic LC as well as ionic smectic glasses (ISG). Every molecule consists of alkyl chains that ended by carboxyl anions, which are connected with one-, di- or ter-valence metal cation. ILCs form a stable bi-layer spatial structure including alkyl chains and anion-cation layers between them. ILCs associate with smectic A. The review [1] gives a broad description of stability, chemical and physical properties of the thermotropic ILC mesophases as well as thermotropic binary and ternary mixtures. ILCs possess high intrinsic ionic conductivity that depends on the temperature exponentially. It was noted ILCs exhibit anisotropy of the electric conductivity determined by their bi-layer spatial structure.

Pure lyotropic ILC matrix is transparent in the visible range of spectra. But, because of its amphiphilic nature, various light-absorbing both organic and non-organic impurities can be solved in ILC matrix including polymethine dyes, electro-chromic and photochromic impurities (viologens). At the same time, thermotropic ILC and ISG based on di-valent ion Co^{2+} are coloured and absorb light in the visible spectral range [2]. The coloured ILC and ISG possess the property of dynamic holographic recording based on the resonance nonlinearity of photosensitive centres [3]. At the same time, ILC matrix provides fast relaxation of accumulated heat energy in cells. The characteristic erasure time of residual thermal gratings is ~30 μs at the grating period 15 μm. Heat-conductive properties of ILC matrixes allow one to create composite cells that includes both absorbed photosensitive layers and ILC layers. Thus, dynamic grating recording with fast erasure time was obtained in composite cells containing a polymethine dye film and lyotropic ILC [3]. Note, that the dye film gives only permanent gratings due to creation of a relief on its surface.

Optical holographic recording is studying extensively for molecular LC and polymer-dispersed LC materials exploiting the photorefractive effect [4–5]. Resonance properties of dye dopants have been investigated in different liquid and solid solutions, as well as in polymers [6]. But, usually, the dyes serve as effective light absorbers and nonlinearity are connected with various secondary thermal effects in solvent matrixes. Major efforts are directed to create electrical-controlled memory systems and switching at action of continuous low intensity lasers.

In our investigated ILC composites, the main contribution to nonlinearity is connected with resonance nonlinearity of electronic excited photosensitive centres. The metal-alkanoate ILC matrixes exhibit physical properties (such as a rigid spatial structure, thermal, electrical and dielectrical properties) very similar to solids. Lyotropic

*e-mail: bugaich@iop.kiev.ua

ILC as a heat dissipation layer can be used in composite cell with different dielectric films including complexes with charges transfer, Langmuir-Blodgett dye films. Lyotropic ILCs are like soft electrodes by their electrical properties that are important features to create flexible composite cells. The investigated in this paper ILC based composites can be employed in fast all-optical switching devices under action of picosecond and nanosecond pulses.

We study holographic properties of composite cells based on a polymethine dye film and lyotropic potassium caproate and ISG of the La^{3+} capronate with polymethine dye in the concentration of 0.5 wt.%. The experimental results are explained by developed theoretical modelling the dynamic holography self-diffraction based on the mechanism of absorption saturation.

2. Holographic properties of ILC composites with dyes

Here, we consider optical nonlinearity mechanism of absorption saturation in photosensitive centres in the composite cells based on metal alkanoate ILC. The composite cells contain a polymethine dye thin film covered by a lyotropic ILC layer of the potassium caproate. The dye molecules partially diffuse into ILC matrix, a heterogenous layer being formed between the dye film and the ILC layer. We use the polymethine dye of the anion type, its structural formula is shown in Fig. 1. The thickness of cells is d = 20–30 μm. All the samples have the absorption band in the visible spectrum with the peak close to the wavelength of the laser excitation λ_0 = 539.8 nm. The typical dependence of the optica density D versus the input intensity J of the laser excitation is shown in Fig. 2. This dependence illustrates the brightening effect, and it is approximated by the law

$$D = \frac{D_0}{1 + J/J_s}. \tag{1}$$

The experimental value J_s = 1.4 MW/cm^2, D_0 = 0.66. The ratio of Eq. (1) was obtained from the conventional two-level model that describes electron transitions between the ground excited states at light absorption [7]. This model is usually applied for dye molecules, where the exited state is the lowest from either one or many short-living levels on which the electronic transitions take place during light absorption. Changes of the number of molecules being in the ground state N_1 and on the excited level N_2 is described by the rate equations

$$\begin{aligned} \frac{dN_1}{dt} &= -\gamma\sigma\frac{J}{h\nu}N_1 + \frac{1}{T_1}N_2 \\ \frac{dN_2}{dt} &= \gamma\sigma\frac{J}{h\nu}N_1 - \frac{1}{T_1}N_2 \end{aligned}, \tag{2}$$

where γ is the quantum yield, σ is the absorption cross-section, and $h\nu$ is the photon energy at λ_0, T_1 is the lifetime of the excited level, and J is the light intensity. The total

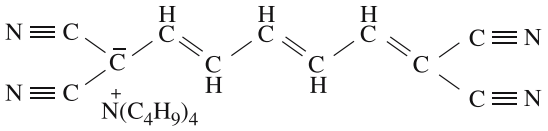

Fig. 1. Structural formula of polymethin anion dye.

amount of the molecules is $N_0 = N_1 + N_2$. Equation (2) has the following solutions

$$\begin{aligned} N_1/N_0 &= n_1^{st}[1 + (J/J_s)\exp(-t(1 + J/J_s)/T_1)], \\ N_2/N_0 &= n_2^{st}[1 - \exp(-t(1 + J/J_s)/T_1)] \end{aligned} \tag{3}$$

where $J_s = h\nu/(\gamma\sigma T_1)$ and

$$\begin{aligned} n_1^{st} &= \frac{N_1^{st}}{N_0} = \frac{1}{1 + J/J_s}, \\ n_2^{st} &= \frac{N_2^{st}}{N_0} = \frac{J/J_s}{1 + J/J_s} \end{aligned} \tag{4}$$

are the population densities of every two levels in the steady state. Equation (4) describes the effect of the absorption saturation. As the optical density is connected with the number of the absorbed molecules by the ratio $D = \sigma N_1 d/\ln(10)$, the experimental ratio in Eq. (1) has the same shape like the first expression in Eq. (4) for n_1^{st}.

For the lyotropic ILC cell (thickness d = 50 μm) with the anion dye of the concentration 0.01 wt.%, we calculate the number of photosensitive molecules $N_0 = 1.4\times10^{17}$ cm^{-3}. From the measured optical density D = 0.43 and using the formula $\sigma = \ln(10)/d\ D/N_0$, we found the absorption cross-section $\sigma = 1.4\times10^{-15}$ cm^2 for the anion dye. The transition time from the excited state to the ground one can be determined from measurements of the fluorescence decay time. For our anion dye, this value is $T_1 = 10^{-11}$ s [8].

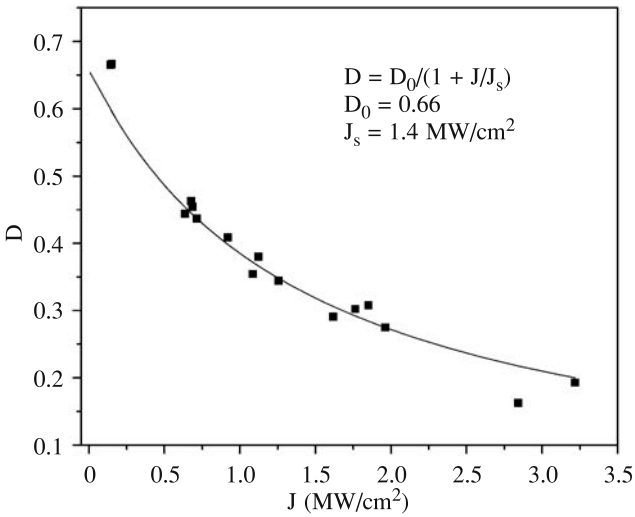

Fig. 2. Changes of the optical density versus the intensity in one laser pulse for composite cell of lyotropic ILC with the anion dye film.

In the course of holographic recording, two input laser beams create an interference pattern. We applied the usual two-wave mixing holographic scheme with transmission geometry. A pumping laser was a double frequency Q-switched Nd:YAP, λ_0 = 539.8 nm, the duration of one pulse was 20 ns, the pulse repetition 3 Hz. In the scheme, the beam from the pumping laser goes through a diaphragm of the diameter of 1 mm and a splitter system, which creates two beams of equal intensities. The beams are converged onto a sample at the angle , which defines the grating period Λ. The output intensity in the regime of the self-diffraction is measured by fast PIN photo-diodes connected with the oscilloscope PCS500 (1 GS/s-50 MHz), and the signals are registered by a computer.

$$\Delta\kappa = \frac{\lambda_0}{4\pi}\sigma N_0(n_2^{st} - n_1^{st}) = \frac{\ln(10)}{4\pi}\frac{\lambda_0}{d}D(n_2^{st} - n_1^{st}). \quad (6)$$

The absorption grating is described in the steady state by Eq. (6). As the grating has a non-sinusoidal profile, the output intensity can be expanded into the Fourier series. As a result, many diffraction orders are observed. The output intensities in every diffracted order can be found from the wave equation [9]. Using the conventional approximation of a slow varying amplitude and taking into account that absorption connected with conduction current is absent during action of a nanosecond laser pulse, we obtain the differential equations followed from the wave equation that describes the changes of the wave complex amplitudes through a nonlinear medium along the direction of light propagation

$$\begin{aligned}
&\frac{d\overline{A}_0}{dz'} = -n_1^{st}D\overline{A}_0 - \frac{1}{2n_0}D[\Delta\kappa^{[1]}(\overline{A}_1 + \overline{A}_{-1}) + \Delta\kappa^{[2]}(\overline{A}_2 + \overline{A}_{-2})] \\
&+i\frac{4\pi}{\ln 10}\frac{d}{\lambda}[\Delta n^{[1]}(\overline{A}_1 + \overline{A}_{-1}) + \Delta n^{[2]}(\overline{A}_2 + \overline{A}_{-2})] \\
&\frac{d\overline{A}_{1,-2}}{dz'} = -n_1^{st}D\overline{A}_{1,-2} - \frac{1}{2n_0}D\Delta\kappa^{[1,2]}\overline{A}_0 + i\frac{4\pi}{\ln 10}\frac{d}{\lambda}\Delta n^{[1,2]}\overline{A}_0 - i\frac{4\pi}{\ln 10}\frac{d}{\lambda}8n_0(\sin\theta)^2\overline{A}_{1,-2}, \\
&\frac{d\overline{A}_{-1}}{dz'} = -n_1^{st}D\overline{A}_{-1} - \frac{1}{2n_0}D\Delta\kappa^{[1]}\overline{A}_0 + i\frac{4\pi}{\ln 10}\frac{d}{\lambda}\Delta n^{[1]}\overline{A}_0 \\
&\frac{d\overline{A}_2}{dz'} = -n_1^{st}D\overline{A}_2 - \frac{1}{2n_0}D\Delta\kappa^{[2]}\overline{A}_0 - i\frac{4\pi}{\ln 10}\frac{d}{\lambda}\Delta n^{[2]}\overline{A}_0 - i\frac{4\pi}{\ln 10}\frac{d}{\lambda}24n_0(\sin\theta)^2\overline{A}_2
\end{aligned} \quad (7)$$

The input intensity distribution can be described by a sinusoidal function on the cell plane

$$J(x) = 2J_0(1 + \cos(Kx)), \quad (5)$$

where J_0 is the intensity of one beam, $K = 2\pi/\Lambda = 4\pi\sin\theta/\lambda_0$ is the grating period, x is the direction on the cell plane, and z is the direction of light propagation along the cell thickness. Equation (5) is valid for equal intensities of the both input laser beams. Due to the nonlinear effect of the absorption saturation, the distribution profile of the absorbed molecules will not coincide with the intensity profile of Eq. (5) inside the cell.

The brightening effect connected with the absorption saturation manifest itself in a change of the cell transmission, which can be described by the Lambert-Bouguer law $I_d/I_0 = \exp(-\Delta N\sigma d)$, where I_d is the output light intensity from a sample of the thickness d, and I_0 is the input intensity. The absorption constant $\alpha = \Delta N\sigma$ is defined by the difference between the number of molecules being in the excited state and in the ground one. Further, we use the definition of the complex refractive index $\hat{n} = n + i\kappa$, the relation between α and the absorption index $\kappa = \alpha/(2k_0) = \alpha\lambda/(4\pi)$ and the ratio for the optical density after illumination in the steady state $D = dN_0\sigma/\ln(10)$. Then, we can express the absorption index modulation through the values of D and population densities

where $\overline{A}_i = A_i\exp(\varphi_i)$ is the wave complex amplitude, $i = \pm1, \pm2$ designates the diffraction orders, $i = 0$ denotes the transmission beam, $z' = z/d\ \ln 10/2\cos\theta$ is the normalized coordinate, n_0 is the average refractive index (for the potassium caproate n_0 = 1.44). In the second equation, one has to use either the first indexes before the comma for the wave of the first diffraction order or the second indexes for the minus-second diffracted order. Equation (7) describes the diffraction from a given grating that can apply to study the self-diffraction regime in thin non-volumetric samples. Also, we restrict our consideration only by two diffraction orders. The first term in the every part of Eq. (7) is the light absorption, the second term is the diffraction from the absorption grating $\Delta\kappa$, the third term is the diffraction from the refractive index grating Δn, $\Delta\kappa^{[m]}$ *and* $\Delta n^{[m]}$ *marks the m-th Fourier component of the corresponding gratings. The fourth terms in Eq. (7) designate a phase incursion, which a wave takes when propagating in the direction of a definite diffraction order. The modulation of the refractive index is connected with the absorption grating by the Kramers-Kronig relationship*

$$\Delta n^{[m]} = \frac{\ln 10}{4\pi}\frac{\lambda_0}{d}D(n_2^{st[m]} - n_1^{st[m]}) \times \frac{2}{\pi}\int D(\lambda)\frac{d\lambda'}{\lambda'[1 - (\lambda'/\lambda_0)^2]}, \quad (8)$$

where $D(\lambda)$ is the normalized absorption spectral band, n_1^{st} and n_2^{st} are calculated from Eq. (4), and λ_0 is the wavelength of the holographic registration, in our case of the self-diffraction λ_0 = 539.8 nm. For the self-diffraction the output intensity in the first diffraction order J_1^{out} is the interference between the first order and the minus-second order of the two output waves

$$J_1^{out} = \left|\overline{A}_1 + \overline{A}_{-2}\right|^2 = I_1 + I_{-2} + 2A_1A_{-2}\cos(\varphi_1 - \varphi_{-2}) \quad . \qquad (9)$$

The typical measured dependence of the J_1^{out} versus energy of the laser beam is presented in Fig. 3 for the composite cell of lyotropic ILC with the anion dye film. Similar curves were obtained for ionic smectic glasses with the dye. The calculation of the diffraction efficiency with taking into consideration only the absorption grating $\Delta\kappa$ shows, that the experimental diffraction efficiency is four orders higher as compared with the calculated one. In this case, the main influence on the holographic recording is caused by the refraction index modulation. The continuous curve in Fig. 3 is the theoretical fitting made from Eq. (7) with including into consideration the refraction index grating. The meaning of the Kramers-Kronig integral served as the fitting parameter. These experimental and theoretical dependences show that the proposed model can be applied to explain the observed holographic efficiency in the Raman-Nath self-diffraction regime.

3. Temporal relaxation of the ILC matrix

A distinctive feature of the holographic recording in composites with metal alkanoate ILC is that the ILC matrix provides fast temporal relaxation of created thermal gratings. Actually, the optical nonlinearity results from the resonance nonlinearity at light absorption by photosensitive centres of composites. The absorbed energy due to non-radiative transitions from excited states to the ground state leads to a local heating that creates expansion or stress of the material and, in such a manner, induces thermal gratings [7]. The thermal gratings often give the main effect on the refraction index modulation for majority classes of holographic LC materials. But, for metal alkanoate ILC, the thermal gratings fast disappear after termination of a pumping laser pulse.

To study relaxation processes in the dynamics gratings, the scheme with a probe beam from a Nd:YAP laser was used for grating readout. The intensity of the probe beam was two orders smaller as compared with that of writing beams. We arranged the set-up with a time delay for the probe beam readout relatively to the beginning of the writing pulse. The maximum delay time was 50 ns. The experimental results show that the diffraction efficiency over 30 ns after the end of the writing pulse is decreased approximately three-fold. We suggest that the induced nonlinearity in the time region later on the termination of the acting laser pulse is connected with the arising thermal grating. The corresponding Δn can be caused by elastic deformation due to local heating in the ILC. The properties of ILC viscous smectic matrix are similar to solids but not to solutions, and heating leads to elastic deformation mainly in ILC.

Time relaxation of weak residual thermal gratings in our holographic set-up was investigated as well. The grating was indicated using a probe beam from a He-Ne laser that had the intensity 2 mW. The registration of the output intensity in the first diffraction order started from the time t = 10 μs after launching nanosecond laser pulse. The typical relaxation kinetics for the probe beam is shown in Fig. 4. The time constant for the thermal grating relaxation is $\tau_{th} \approx 57$ μs for La-capronate ISG. The relaxation process of non-equilibrium heat distribution can be described by the conventional heat equation, which has an exponential form with the characteristic time constant [10]

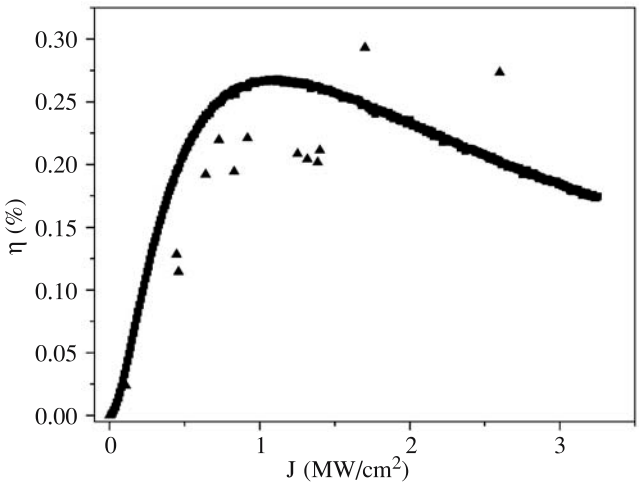

Fig. 3. Measured self-diffraction efficiency in the first order versus the intensity of the input laser pulse for lyotropic composite cells with the anion dye film. The solid curve is the theoretical calculations with the fitting parameter In(λ) = 0.225.

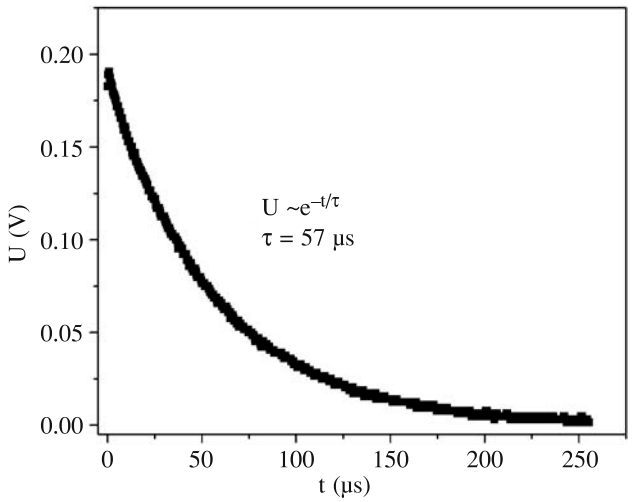

Fig. 4. Time relaxation kinetics of the probe beam intensity in the first diffraction order for the cell with the smectic glass $La(C_5H_{11}COO)_3$ doped by anion dye (0.5 wt.%).

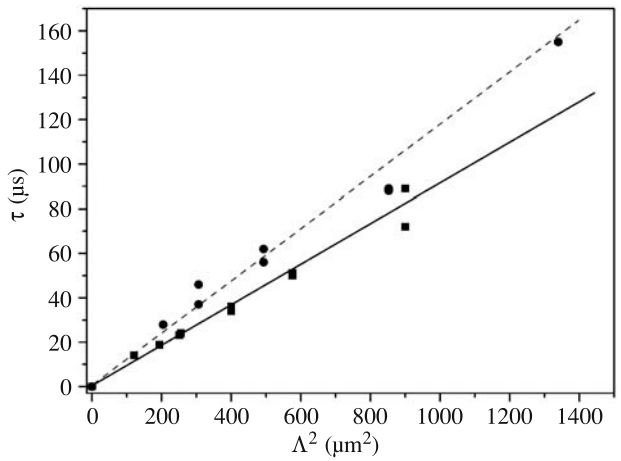

Fig. 5. Decay time constant of the thermal gratings versus the square of the grating period for the lyotropic ILC with the anion dye film (dash line) and for the smectic glass $La(C_5H_{11}COO)_3$ doped by anion dye (0.5 wt.%) (solid line).

$$\tau_{th} = \Lambda^2 / (4\pi^2 D_T). \tag{10}$$

The coefficient of the thermal diffusion D_T is expressed by the ratio $D_T = K_T / (\rho c_p)$, where K_T is the coefficient of thermal conductivity, ρ is the material density, c_p is the specific heat capacity at a constant pressure.

The experimental dependences of the relaxation time constant versus the square of the grating period both for composite cells with lyotropic ILC and for ionic smectic glasses are presented in Fig. 5. One can see that these dependences obey Eq. (10). From the experimental measurements, we determined the diffusion coefficients D_T for the both media. D_T has similar values in lyotropic cells (D_T = 0.0017 cm/s) and in glass cells (D_T = 0.0012 cm/s which means that the mechanism of heat relaxation is defined by the properties of the metal alkanoate matrix. That may be phonons of the smectic ILC lattice that are responsible for the dissipation of weak residual thermal gratings.

4. Conclusions

The main holographic characteristics of the dynamic gratings have been obtained for the composites based on lyotropic ILC of the potassium caproate and of ionic smectic glasses of the La-capronate containing photosensitive polymethine dye of the anion type. The recording of dynamic gratings lasts for the time 20 ns, the erasure does for 100 μs. Ionic smectic matrix provides fast effective heat relaxation in thin composite cells. The optical nonlinearity of the investigated composites is the result of the resonance nonlinearity due to absorption saturation of excited dye molecules. The corresponding theory describing the self-diffraction regime of Raman-Nath thin grating is developed. The comparison of our theory with the experiments shows a good agreement. This theoretical approach can be used for holographic investigations of materials with high changes of the refraction index.

Note, that the resonance nonlinearity besides of absorption saturation (defined by the difference of numbers of molecules being in excited and ground states) includes also the effect connected with changes of the dipole momentum of the electron transition in molecules at light excitation [7]. Then, the refractive index modulation should be supplemented by the component Δn_d followed from the dipole momentum change. In this case, the refraction index modulation and the holographic diffraction efficiency can be significantly increased by using novel materials with giant resonance nonlinearity. For example, miracyanine dyes have the transition dipole momentum 10 times higher as compared with that of ionic polymethine dyes [11].

Further researches of Bragg diffraction in thin films, as well as creation of composite films for other applications, for example for lasing effects, fiber lasers, luminophores, are perspective. Composites based on ILC and ionic smectic glasses can become promising materials for applications in all-optical switch elements for telecommunications systems, in hybrid organic/inorganic photoconductive materials, in bifunctional (electro-optical) cells. The composite cells based on ILC permit one to provide different types of optimization, for example to use the films of novel dye molecules with giant nonlinearity for the purposes of effective real time dynamic holography.

References

1. T.A. Mirnaya, V.D. Prisyajnyuk, and V.A. Shcherbakov, "Liquid crystal state of salt melt with organic ions", *Russian Chemistry Rev.* **58**, 1429–1450 (1989).
2. A.V. Gridyakina, A.P. Polishchuk, and A.V. Koval'chuk, "Physical properties of liquid crystals in lead decanoate systems", *Russian J. Physical Chemistry* **79**, Suppl. 1, S71–S75 (2005).
3. G. Klimusheva, S. Bugaychuk, and Y. Garbovskiy, "Fast dynamic holographic recording based on conductive ionic metal-alknoate liquid crystals and smectic glasses", *Opt. Lett.* **31**, 235–237 (2006).
4. O. Ostroverkhova and W.E. Moerner, "Organic photorefractives: mechanisms, materials, and applications", *Chem. Rev.* **104**, 3267–3314 (2004).
5. G. Wiederrecht, "Photorefractive liquid crystals", *Annu. Rev. Mater. Rev.* **31**, 139–169 (2001).
6. T. Todorov, P. Markovski, N. Tomova, V. Dragostinova, and K. Stoyanova, "Photopolymers – holographic investigations, mechanism of recording and applications", *Optical and Quantum Electronics* **16**, 471–476 (1984).
7. H.I. Eichler, P. Gunter, and D.W. Pohl, *Laser-induced Dynamic Gratings*, Springer-Verlag, Berlin Heidelberg, 1986.
8. A.A. Ishchenko, *Structure and Spectral-luminescent Properties of Polymethine Dyes*, Naukova Dumka, Kiev, 1994. (in Russian)
9. V. Vinetskii, N. Kukhtarev, S. Odoulov, and M. Soskin, "Dynamic self-diffraction of coherent light beams", *Soviet Uspehi Fizicheskih Nauk* **129**, 113–137 (1979). (in Russian)
10. S. Odoulov, M. Soskin, and A. Khyzhnyak, *Dynamic Grating Lasers*, Nauka Publishers, Moscow, 1990. (in Russian)
11. A.D. Kachkovskii, "The nature of electron transition in linear conjugated system", *Russian Chem. Rev.* **66**, 715–734 (1997).